Dipole Moment of a Superatom

B. Yang,[1,†] Y. Li,[1,†] S. Nie,[1,†] Y. Mei,[2] H. Nguyen,[1] P. R. Berman,[1] and A. Kuzmich[1,*]
[1]Department of Physics, University of Michigan, Ann Arbor, Michigan 48109, USA
[2]Department of Physics and Astronomy, Washington State University, Pullman, Washington 99164, USA

(Received 17 April 2024; accepted 2 October 2024; published 19 November 2024)

Homodyne detection is used to measure the (collective) atomic dipole moment for an atomic ensemble that is prepared in a superposition of spatially phased Dicke states having at most two excitations (a so-called "superatom"). Homodyne detection allows one to isolate the contributions to the radiated intensity that depend linearly on the average value of the collective atomic dipole moment operator. Depending on whether the atom-reference field interference is constructive or destructive, either super-Poisson or sub-Poisson statistics for the combined field is observed.

DOI: 10.1103/PhysRevLett.133.213601

Introduction—There has been an ongoing debate over the last 60 years as to the role played by the collective dipole moment operator in theories of superradiance. In one section of his classic paper on superradiance, Dicke considered the radiation emitted by an extended atomic sample following excitation by a short radiation pulse [1]. By calculating the emission pattern of a phased array of atomic dipoles, he found that the signal radiated in the phase-matched direction scales as the square of the number of atoms in the sample. Rehler and Eberly developed a somewhat more complete theory of this superradiant emission, allowing for media having a large optical depth [2]. Using an approximation in which each atom in the ensemble has the same decay dynamics, they found that it is possible to have almost all the energy initially stored in the sample emitted in the phase-matched direction. The quantum-mechanical expectation value of the phase-matched radiated field, denoted by $\langle \hat{E} \rangle$, is nonvanishing for this scenario.

In contrast, experimental protocols involving two-photon decays in a cascade (ladder) level configuration were proposed and implemented [3] in which a shared single excitation among the atoms leads to superradiant emission from the sample, despite the fact that the average value of the dipole moment vanishes. For the radiation to be superradiant, the optical depth of the sample must be large [4,5]. To produce a fully symmetric Dicke state without post selection, it proved advantageous to use level schemes involving Rydberg atoms [6–18].

Scully *et al.* emphasized that the directional phase-matched emission radiated by an atomic ensemble in which the atoms share a single, phased excitation [19] was produced despite the fact that the dipole moment of the ensemble vanishes identically and $\langle \hat{E} \rangle$ of the radiated field is equal to zero. In other words, the spatial phase imprinted on the atoms by the excitation field is the critical ingredient required for superradiant, phase-matched emission, a conclusion shared by Eberly [20].

That is, there is no reason to believe, *a priori*, that a nonvanishing average dipole moment operator is needed for superradiant emission, since the radiated intensity depends on the expectation value of the product of collective dipole operators rather than on the average value of the dipole moment operator itself. It is only in a scheme such as that considered by Rehler and Eberly or those considered in traditional theories of optical coherent transients [21–25], where the expectation value of the product of dipole operators is equal to a product of the expectation values, that a nonvanishing expectation value is required.

On the other hand, if one mixes the atomic output with a reference field, the field-ensemble interference term serves as a measure of the average value of the collective dipole operator. This term would contribute if the atoms are prepared in an unentangled factorized state but would vanish if the atoms are prepared in a pure Dicke state. Moreover, since the interference term is proportional to the expectation value of the dipole moment operator, a phase-dependent measurement of the field also serves as a measurement of the atomic dipole moment.

In this Letter, we investigate the collective atomic dipole moment for a strongly-interacting atomic ensemble using homodyne detection with a reference field. Using two-photon laser excitation in resonance between the ground and Rydberg states, an ensemble of atoms is prepared in a state that can be described as a superposition of Dicke states having zero ($n = 0$), one ($n = 1$), and two ($n = 2$) atomic excitations. A retrieval pulse then maps this excitation onto a state that is radiatively connected to the ground state (see Fig. 1). The advantage of this excitation scheme is that a collective state can be prepared across the entire sample,

*Contact author: akuzmich@umich.edu
†These authors contributed equally to this work.

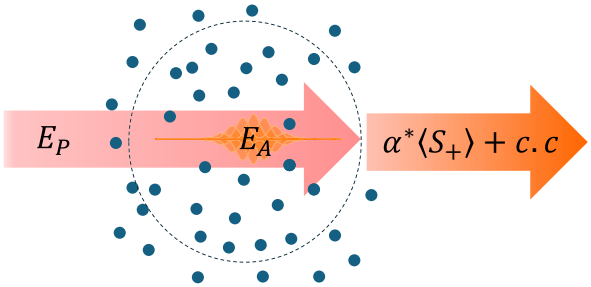

FIG. 1. Laser fields E_1 and E_2 (not shown) induce excitations within an ensemble of ^{87}Rb atoms. A readout field then leads to phase-matched atomic emission E_A, which is proportional to the expectation value $\langle S_+\rangle$ of the collective atomic lowering operator. A classical probe field E_P having amplitude α and phase ϕ spatially overlaps and interferes with E_A. Interference terms scaling linearly with $\langle S_+\rangle$ can be isolated from the combined intensity measured at a detector and serve as a measure of the collective dipole moment of the ensemble.

since the excitation pulse undergoes negligible absorption as it traverses the sample. Depending on whether the interference between the atomic and reference fields is constructive or destructive, the combined field is characterized by either super-Poisson or sub-Poisson statistics.

While our focus is on how quantum correlations between atoms affect the dipole moment, related single-atom effects were investigated by Thomas and coworkers who employed heterodyne detection of atomic fluorescence to study its phase-dependent properties [26], quadrature squeezing [17,27], and atomic noise [28], while heterodyne measurements of a single-ion fluorescence were used to confirm that the elastically scattered light (and, therefore, the ion's dipole moment) are coherent with the driving laser field [29,30].

Experimental protocol—An ensemble of ~900 ultracold ^{87}Rb atoms is prepared in a state-insensitive trap for the $5s - 75s$ transition of our experiment. The longitudinal waist of the atomic cloud is ~10 μm along the excitation beam direction, and the transverse waist of the atomic cloud is ~6 μm defined by the excitation beam waist. The atoms are optically pumped into the ground state $|g\rangle = |5S_{1/2}, F = 2, m_F = -2\rangle$, with the state of the ensemble described by a product state, $|\mathbf{0}\rangle = |g_1, \ldots, g_N\rangle$. The atoms are then coherently driven from the ground state $|g\rangle$ to the Rydberg state $|r\rangle = |75S_{1/2}, m_J = -1/2\rangle$ by laser fields E_1 and E_2 with duration T_p and detuning of $\delta = 2\pi \times 20$ MHz from the intermediate state $|e\rangle = |5P_{3/2}, F = 3, m_F = -3\rangle$.

Owing to the combined action of the Rydberg blockade and the interaction-induced dephasing, the state vector is truncated to include at most two excitations in the following form $|\Psi\rangle = \beta_0|\mathbf{0}\rangle + \beta_1|\mathbf{1}\rangle + \beta_2|\mathbf{2}\rangle$ [31,32], where $|\mathbf{1}\rangle$ and $|\mathbf{2}\rangle$ represent symmetric Dicke states having one and two excitations, respectively, defined as $S_+|\mathbf{0}\rangle = |\mathbf{1}\rangle$ and $S_+|\mathbf{1}\rangle = \sqrt{2}|\mathbf{2}\rangle$, in the large N approximation. The operator $S_\pm$ is given by $S_\pm = (1/\sqrt{N})\sum_{j=1}^{N}\sigma_\pm^{(j)}$, with $\sigma_\pm^{(j)}$ being the raising and lowering operators for atom j. Spatial phase factors have been suppressed since they will not contribute in the phase-matched direction.

Following a storage period of $T_s \simeq 0.3$ μs, the atoms are driven by a (σ^+-polarized) retrieval field E_R resonant on the $|r\rangle \leftrightarrow |e\rangle$ transition. This process creates an array of atomic dipoles leading to a phase-matched emission E_A from the sample. For sufficiently small ensembles and/or high principal quantum numbers, the $n = 2$ Dicke state does not measurably contribute to the retrieved light, E_A. This is indicated by the second order correlation function for E_A, $g_A^{(2)}(0) \equiv (\langle E_-E_-E_+E_+\rangle/|\langle E_-E_+\rangle|^2)$ being close to zero [8,14]. However, in this experiment, the combination of ensemble size, the principal quantum number of the Rydberg state, and the storage time are such that there is an admixture of the $n = 2$ Dicke state. As a consequence, there is a contribution to the expectation value of the atomic dipole moment operator between both the ($n = 2$ and $n = 1$) and the ($n = 0$ and $n = 1$) components of the state vector. We are able to separate these contributions experimentally.

The emitted field E_A is spatially and temporally overlapped with a probe pulse E_P, as in the scheme shown in Fig. 1, within a ~60 ns time window. The probe pulse E_P is tuned to have the same frequency as E_A. The combined field is then split by a polarizing beam splitter and directed into two single-mode optical fibers coupled to the single-photon-counting modules (SPCMs), forming a Hanbury Brown–Twiss (HBT) setup [33–35].

Theoretical model—In dimensionless units, the electric field operator at the position of the detector, $E_- = \alpha^* + B\sqrt{N}S_+$, is a sum of the classical probe field amplitude and atomic source field operator [36,37], where $\alpha = |\alpha|e^{i\phi_\alpha}$ is a complex number characterizing the intensity and phase of the probe field E_p at the detectors and B is effectively the cooperativity of the sample. For perfect spatial and temporal overlap of the probe and atomic fields, the field intensity incident on the detectors, integrated over the time window containing both field pulses, is given by $I_T = \int dt\langle E_-E_+\rangle$, where $E_+ = E_-^\dagger$, and the second order correlation function by $g^{(2)}(0) = A_T/I_T^2$, where $A_T = \int dt\langle E_-E_-E_+E_+\rangle$. For simplicity, we define $g^{(2)} \equiv g^{(2)}(0)$.

We account for the temporal overlap and spectral phase noise between E_A and E_P using a coefficient ξ described in Supplemental Material [38]. It then follows that the intensity is given by

$$\frac{I_T}{|\alpha|^2} = 1 + f^2(1 + 2s|\beta_1|^2) + 2f\xi\left(\beta_0\cos\phi + \sqrt{s}|\beta_1|^2\cos(\phi + \phi')\right), \quad (1)$$

and A_T by

$$\frac{A_T}{|\alpha|^4} = 1 + 2f^2(1 + s|\beta_1|^2)(1 + \xi^2) + f^4 s + 4f\xi\left(\beta_0 \cos\phi + \sqrt{s}|\beta_1|^2 \cos(\phi + \phi')\right) + 2f^2\xi^2\beta_0\sqrt{s}\cos(2\phi + \phi') + 4f^3\xi\sqrt{s}\cos(\phi + \phi'), \quad (2)$$

where we define $f \equiv B\sqrt{N}|\beta_1|/|\alpha|$ as the ratio between the emission and probe field amplitudes, and $s \equiv 2|\beta_2|^2/|\beta_1|^4$ as the value of $g^{(2)}$ associated with the source field. There are two phases that enter these expressions: $\phi \equiv \phi_1 - \phi_\alpha$ is the phase between the $n = 1$ Dicke state and the probe field, which is introduced by the controllable phase between E_1 and E_P, and $\phi' \equiv \phi_2 - 2\phi_1$ is the interaction-induced phase difference, which measures the phase shift in the $n = 2$ Dicke state due to the Rydberg interaction. The terms varying as $\cos\phi$ originate from coherence between states ($n = 0$ and $n = 1$), those varying as $\cos(\phi + \phi')$ from coherence between states ($n = 2$ and $n = 1$), and those varying as $\cos(2\phi + \phi')$ from coherence between states ($n = 0$ and $n = 2$).

Equation (1) predicts a sinusoidal interference pattern with destructive interference approximately at $\phi \approx \pi$. In scenarios where $f \sim 1$, we also expect to observe a peak in the second-order correlation function $g^{(2)}$ at the point of destructive interference ($\phi = \pi$). In the context where only the $n = 0$ and $n = 1$ Dicke states are considered, Eqs. (1) and (2) can be simplified by setting s to zero. In this limit, the visibility $\mathcal{V}$ of the interference fringe and the maximum value of $g^{(2)}$ at the lowest point of the fringe, $g^{(2)}_{\max}$, are given by

$$\mathcal{V} = \frac{2f\beta_0}{1 + f^2}, \quad (3a)$$

$$g^{(2)}_{\max} = \frac{1 + 4f^2 - 4f\beta_0}{(1 + f^2 - 2f\beta_0)^2}. \quad (3b)$$

Experimental results—Figure 2(a) shows the observed interference fringe for the photoelectric detection event probability per trial P as a function of phase ϕ. The data are in agreement with our theoretical model when contributions to the collective dipole moment of both singly- and doubly-excited states are included, providing evidence for the phase-coherent nature of the collective dipole moment beyond the regime of single excitation. Notably, at $\phi = \phi_{\max} = 200°$, we observe a minimum in the photoelectric detection probability with $P = 0.002$. This minimum is different from the theoretical minimum at $\phi = 180°$ due to the experimental phase offset, ϕ_0, which is mainly due to the optical path difference between the excitation and probe fields.

In Fig. 2(b), the measured values of $g^{(2)}$ exhibit either photon bunching and antibunching depending on the value of ϕ. When the probe field and emission field destructively

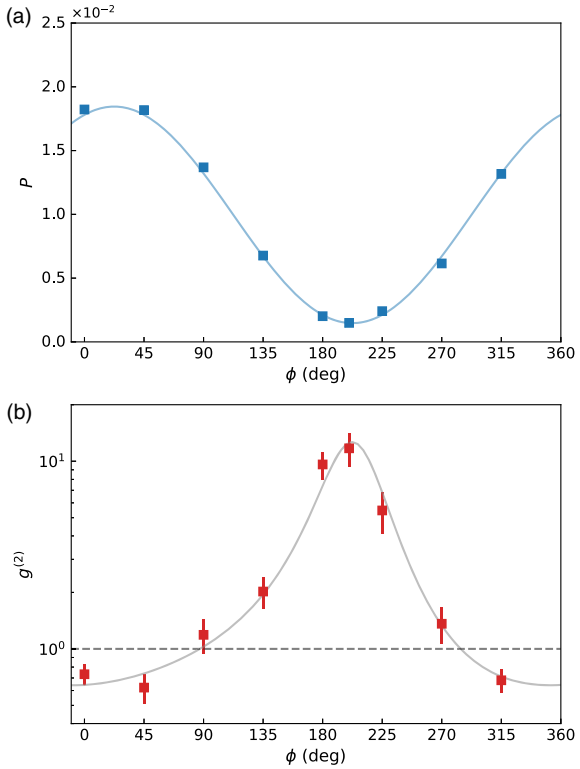

FIG. 2. Photoelectric detection event probability per trial P and second-order correlation function $g^{(2)}$ as a function of the relative phase ϕ between the $n = 1$ Dicke state and the probe field. (a) Sum of detection count rates at D_1 and D_2 shows an interference fringe with visibility $\mathcal{V} \approx 0.85 \pm 0.03$ (blue solid curve). The error bars are smaller than the size of plot markers. (b) The measured values of $g^{(2)}$, with the theoretical (gray solid) curve based on theory with no fitting parameters.

interfere, a pronounced bunching is observed. This corresponds to the nearly complete destructive interference between the Poisson components of the atomic and the probe field, therefore isolating the contribution of the doubly-excited collective atomic state [37]. The highest value of the second-order correlation function $g^{(2)}$ is $g^{(2)}_{\max} = 11.7 \pm 2.4$, while, under the condition of constructive interference, the observed antibunching effect of $g^{(2)} \sim 0.5$ can be understood as being a result of an equal mixture of Poissonian probe with $g^{(2)} \approx 1$ and an (approximately) single-photon emission with $g^{(2)} \approx 0$.

It is important to note the slight asymmetry in Fig. 2(b), where the plot appears skewed to the left. This asymmetry is ascribed to the presence of two-photon components in the atomic emission. In an ideal scenario where s is exactly zero, the $g^{(2)}$ distribution would be perfectly symmetric around its peak. However, in our experiment, the presence of ϕ' and s introduces additional components to A_T for $\phi < \phi_{\max}$, resulting in the left-skewed appearance in Fig. 2(b). Calculating the dynamic $g^{(2)}$ and interaction-induced phase shift after the storage period T_s yields

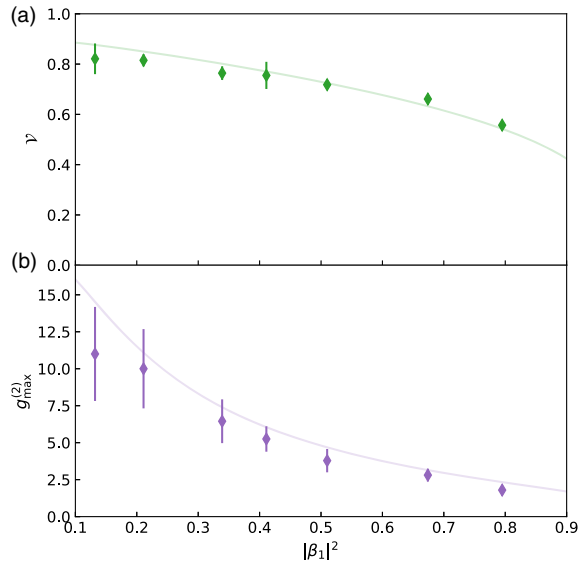

FIG. 3. Visibility $\mathcal{V}$ of the interference fringe (a) and $g^{(2)}_{\max}$ (b) as a function of the single-excitation probability $|\beta_1|^2$. The value of $|\beta_1|^2$ is controlled and estimated by the length of the excitation pulse T_p. Both the visibility and $g^{(2)}_{\max}$ decrease with increasing $|\beta_1|^2$. The vertical error bars in (a) are extracted from the fitting of the interference fringes. The solid curves are based on the theory model.

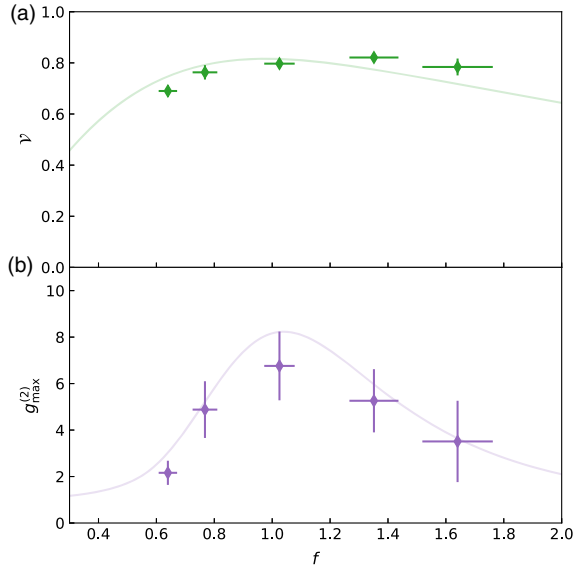

FIG. 4. Visibility $\mathcal{V}$ of the interference fringe (a) and $g^{(2)}_{\max}$ (b) as a function of emission-probe ratio f using $T_p = 0.2$ μs. The solid curves are based on the theory model.

$\phi' = -0.3\pi$ and $s = 0.12$ at $n = 75$ [35,38], which we employ as fixed parameters for our theoretical model. The negative sign of ϕ' is indicative of the repulsive nature of the Rydberg interactions in our system.

A notable feature of the dipole moment for a two-level system, either a single atom or a superatom, is that it vanishes when all the atoms are in their ground states and when all the atoms are completely inverted. The degree of inversion is a function of parameter $|\beta_1|$ in our model. In Eqs. (3a) and (3b), both the visibility, $\mathcal{V}$, and the maximum of the second order correlation function, $g^{(2)}_{\max}$, depend implicitly on the value of $|\beta_1| \approx \sqrt{1-\beta_0^2}$. We vary $|\beta_1|$ by changing the pulse widths of the excitation fields E_1 and E_2, given the many-body Rabi oscillation [9,34,38]. Subsequently, we calculate the visibility of the interference fringe through a sinusoidal fit and record the highest value of $g^{(2)}$ observed as $g^{(2)}_{\max}$. As shown in Fig. 3, an increase in the single-excitation rate $|\beta_1|^2$ correlates with a decrease in both visibility and $g^{(2)}_{\max}$, consistent with the predictions of Eq. (3).

The visibility of the interference fringe and the $g^{(2)}_{\max}$ is also sensitive to the amplitude ratio f between the emission field E_A and the probe field E_P. In Figs. 4(a) and 4(b), we demonstrate the effects of varying f by adjusting the intensity of the probe pulse while maintaining a constant value for $|\beta_1|^2$. In this set of experimental trials, we select $T_p = 0.2$ μs, which corresponds to $|\beta_1|^2 = 0.30$, a value intentionally chosen to be higher than that used in Fig. 2(b) in order to reduce measurement time for $g^{(2)}$. Consequently, $g^{(2)}_{\max}$ in Fig. 4(b) is observed to be lower than that in Fig. 2. We found that both the visibility and $g^{(2)}_{\max}$ reach their peak values when the probe and emission fields are balanced in amplitude at $f \approx 1$, a conclusion in agreement with Eqs. (3a) and (3b). Likewise, when the probe field and emission field are imbalanced in amplitude, the imperfect cancellation between the fields leads to a reduction in both $\mathcal{V}$ and $g^{(2)}_{\max}$ from $f = 1$. In fact, when $f \to 0$, the probe field E_P dominates, leading to $\mathcal{V} \to 0$ and $g^{(2)} \to 1$; when $f \to \infty$, the emission field E_A dominates, leading to $\mathcal{V} \to 0$ and $g^{(2)} \to s$ (for $|\beta_1|^2 \gg 2|\beta_2|^2$).

Conclusion—If atoms are viewed as classical oscillators, superradiant emission can occur only if the dipole moments of the oscillators are nonvanishing and only if the contributions from the oscillators interfere constructively. Of course, atomic dipoles are not classical dipoles. In the case of an atomic ensemble of two-level atoms, superradiance can occur even when the dipole moment of each atom vanishes, provided the atoms are prepared in a state having spatial phase coherence. Thus, there is no debate as to whether or not a nonvanishing dipole moment is needed for atoms to undergo superradiant emission.

In our experiment we have observed phase-dependent properties for the field emitted by an ensemble of atoms prepared in a superposition of the ground and the two lowest-excited Dicke states. The interference effects in the field intensity and $g^{(2)}$ can be interpreted in terms of the dipole moment contributions of the singly- and doubly-excited state components. By tuning the relative phase between these two fields, the combined field is bunched or

anti-bunched when destructive or constructive interference occurs, respectively. In the absence of the reference field, both the intensity and the second order correlation functions of the field radiated by the atoms depend only on collective state populations. It is only by using homodyne detection that we can generate a signal that depends on both the populations and coherences (that is, a nonvanishing dipole moment) of the Dicke states.

Acknowledgments—This work was supported by the Air Force Office of Scientific Research and the National Science Foundation.

[1] R. H. Dicke, Coherence in spontaneous radiation processes, Phys. Rev. **93**, 99 (1954).
[2] N. E. Rehler and J. H. Eberly, Superradiance, Phys. Rev. A **3**, 1735 (1971).
[3] T. Chanelière, D. N. Matsukevich, S. D. Jenkins, T. A. B. Kennedy, M. S. Chapman, and A. Kuzmich, Quantum telecommunication based on atomic cascade transitions, Phys. Rev. Lett. **96**, 093604 (2006).
[4] P. R. Berman and J.-L. Le Gouet, Absorption of a pulse by an optically dense medium: An argument for field quantization, Am. J. Phys. **79**, 527 (2011).
[5] P. R. Berman and J.-L. Le Gouet, Phase-matched emission from an optically thin medium following one-photon pulse excitation: Energy considerations, Phys. Rev. A **83**, 035804 (2011).
[6] M. D. Lukin, M. Fleischhauer, R. Cote, L. M. Duan, D. Jaksch, J. I. Cirac, and P. Zoller, Dipole blockade and quantum information processing in mesoscopic atomic ensembles, Phys. Rev. Lett. **87**, 037901 (2001).
[7] M. Saffman and T. G. Walker, Creating single-atom and single-photon sources from entangled atomic ensembles, Phys. Rev. A **66**, 065403 (2002).
[8] Y. O. Dudin and A. Kuzmich, Strongly interacting Rydberg excitations of a cold atomic gas, Science **336**, 887 (2012).
[9] Y. O. Dudin, L. Li, F. Bariani, and A. Kuzmich, Observation of coherent many-body Rabi oscillations, Nat. Phys. **8**, 790 (2012).
[10] L. Li, Y. O. Dudin, and A. Kuzmich, Entanglement between light and an optical atomic excitation, Nature (London) **498**, 466 (2013).
[11] D. Maxwell, D. J. Szwer, D. Paredes-Barato, H. Busche, J. D. Pritchard, A. Gauguet, K. J. Weatherill, M. P. A. Jones, and C. S. Adams, Storage and control of optical photons using Rydberg polaritons, Phys. Rev. Lett. **110**, 103001 (2013).
[12] L. Li and A. Kuzmich, Quantum memory with strong and controllable Rydberg-level interactions, Nat. Commun. **7**, 13618 (2016).
[13] H. Busche, P. Huillery, S. W. Ball, T. Ilieva, M. P. A. Jones, and C. S. Adams, Contactless nonlinear optics mediated by long-range Rydberg interactions, Nat. Phys. **13**, 655 (2017).
[14] D. P. Ornelas-Huerta, A. N. Craddock, E. A. Goldschmidt, A. J. Hachtel, Y. Wang, P. Bienias, A. V. Gorshkov, S. L. Rolston, and J. V. Porto, On-demand indistinguishable single photons from an efficient and pure source based on a Rydberg ensemble, Optica **7**, 813 (2020).
[15] S. Shi, B. Xu, K. Zhang, G. S. Ye, D. S. Xiang, Y. Liu, J. Wang, D. Su, and L. Li, High-fidelity photonic quantum logic gate based on near-optimal Rydberg single-photon source, Nat. Commun. **13**, 4454 (2022).
[16] G. S. Ye, B. Xu, Y. Chang, S. Shi, T. Shi, and L. Li, A photonic entanglement filter with Rydberg atoms, Nat. Photonics **17**, 538 (2023).
[17] V. Magro, J. Vaneecloo, S. Garcia, and A. Ourjoumtsev, Deterministic freely propagating photonic qubits with negative Wigner functions, Nat. Photonics **17**, 688 (2023).
[18] A. Paris-Mandoki, Ch. Braun, J. Kumlin, Ch. Tresp, I. Mirgorodskiy, F. Christaller, H. P. Büchler, and S. Hofferberth, Free-space quantum electrodynamics with a single Rydberg superatom, Phys. Rev. X **7**, 041010 (2017).
[19] M. O. Scully, E. S. Fry, C. H. Raymond Ooi, and K. Wodkiewicz, Directed spontaneous emission from an extended ensemble of N atoms: Timing is everything, Phys. Rev. Lett. **96**, 010501 (2006).
[20] J. H. Eberly, Emission of one photon in an electric dipole transition of one among N atoms, J. Phys. B **39**, S599 (2006).
[21] N. A. Kurnit, I. D. Abella, and S. R. Hartmann, Observation of a photon echo, Phys. Rev. Lett. **13**, 567 (1964).
[22] R. G. Brewer and R. L. Shoemaker, Photon echo and optical nutation in molecules, Phys. Rev. Lett. **27**, 631 (1971).
[23] R. G. Brewer and R. L. Shoemaker, Optical free induction decay, Phys. Rev. A **6**, 2001 (1972).
[24] T. Mossberg, A. Flusberg, R. Kachru, and S. R. Hartmann, Tri-level echoes, Phys. Rev. Lett. **39**, 1523 (1977).
[25] P. R. Berman and D. G. Steel, Coherent optical transients, in *Handbook of Optics* (McGraw-Hill, New York, 2010), Vol. 4, Chap. 11.
[26] H. Z. Zhao, Z. H. Lu, and J. E. Thomas, Phase-dependent resonance fluorescence and time ordering in photodetection, Phys. Rev. Lett. **79**, 613 (1997).
[27] Z. H. Lu, S. Bali, and J. E. Thomas, Observation of squeezing in the phase-dependent fluorescence spectra of two-level atoms, Phys. Rev. Lett. **81**, 3635 (1998).
[28] A. M. Bacon, H. Z. Zhao, L. J. Wang, and J. E. Thomas, Optical dipole noise of two-level atoms, Phys. Rev. Lett. **75**, 1296 (1995).
[29] J. T. Höffges, H. W. Baldauf, T. Eichler, S. R. Helmfrid, and H. Walther, Heterodyne measurement of the fluorescent radiation of a single trapped ion, Opt. Commun. **133**, 170 (1997).
[30] Ch. Raab, J. Eschner, J. Bolle, H. Oberst, F. Schmidt-Kaler, and R. Blatt, Motional sidebands and direct measurement of the cooling rate in the resonance fluorescence of a single trapped ion, Phys. Rev. Lett. **85**, 538 (2000).
[31] P. R. Berman and A. Kuzmich, Interplay of the Rydberg blockade and interaction-induced dephasing in Rydberg single-photon sources, Phys. Rev. A **109**, 013710 (2024).
[32] F. Bariani, Y. O. Dudin, T. A. B. Kennedy, and A. Kuzmich, Dephasing of multiparticle Rydberg excitations for fast entanglement generation, Phys. Rev. Lett. **108**, 030501 (2012).
[33] J. Lampen, A. Duspayev, H. Nguyen, H. Tamura, P. R. Berman, and A. Kuzmich, Hanbury Brown-Twiss

correlations for a driven superatom, Phys. Rev. Lett. **123**, 203603 (2019).
[34] Y. Mei, Y. Li, H. Nguyen, P. R. Berman, and A. Kuzmich, Trapped alkali-metal Rydberg qubit, Phys. Rev. Lett. **128**, 123601 (2022).
[35] Y. Li, Y. Mei, H. Nguyen, P. R. Berman, and A. Kuzmich, Dynamics of collective-dephasing-induced multiatom entanglement, Phys. Rev. A **106**, L051701 (2022).
[36] P. R. Berman and V. S. Malinovsky, *Principles of Laser Spectroscopy and Quantum Optics* (Princeton University Press, Princeton, NJ, 2011).
[37] P. R. Berman, H. Nguyen, Y. Mei, Y. Li, and A. Kuzmich, Interference bunching and antibunching of coherent and atomic radiation fields, Phys. Rev. A **108**, 043713 (2023).
[38] See Supplemental Material at http://link.aps.org/supplemental/10.1103/PhysRevLett.133.213601 for more theoretical and experimental details, which includes Ref. [39].
[39] G. M. Stéphan, T. T. Tam, S. Blin, P. Besnard, and M. Têtu, Laser line shape and spectral density of frequency noise, Phys. Rev. A **71**, 043809 (2005).